

1 **Supplementary Material**

2
3
4 **Influence of Dilution System and Electrical Low Pressure Impactor**
5 **Performance on Particulate Emission Measurements from a**
6 **Medium-scale Biomass Boiler**

7
8 **Jordi F. P. Cornette¹, Thibault Coppieters¹, Dominique Desagher²,**
9 **Jurgen Annendijck², H el ene Lepaumier², Nathalie Faniel², Igor Dyakov³,**
10 **Julien Blondeau¹, Svend Bram¹**

11
12 ¹ *Thermo and Fluid Dynamics (FLOW), Vrije Universiteit Brussel (VUB), Pleinlaan 2, 1050*
13 *Brussels, Belgium.*

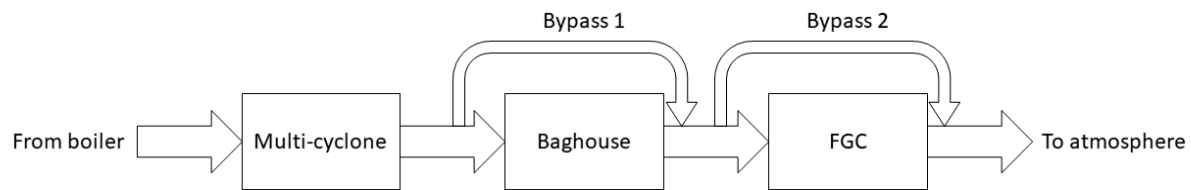
14 ² *Laborelec, ENGIE, Rodestraat 125, 1630 Linkebeek, Belgium.*

15 ³ *Cellule Emissions Atmosph eriques, Institut Scientifique de Service Public (ISSeP), Rue du*
16 *Ch era 200, 4000 Li ege, Belgium.*

17

Corresponding author. Tel: +32 496 085 499

E-mail address: jordi.cornette@vub.be



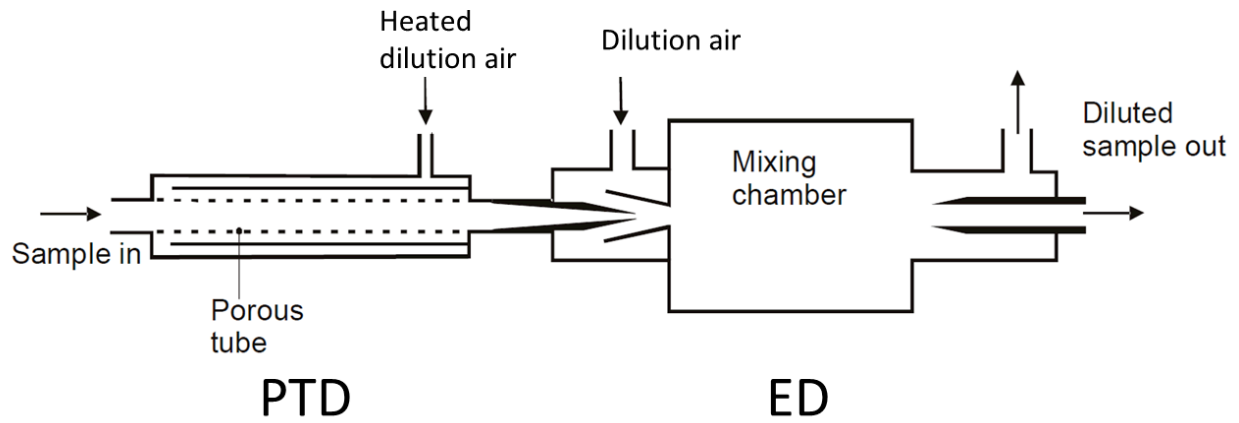
18

19 **Fig. S1.** Schematic representation of the pathway of the flue gas from boiler to atmosphere. FGC:

20 flue gas condenser.

21

22

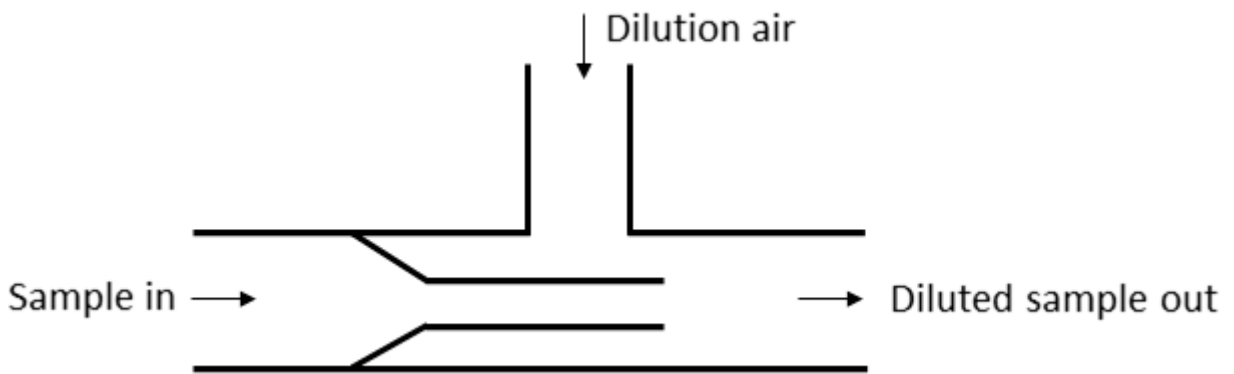


23

24 **Fig. S2.** Two stage dilution system: porous tube diluter (PTD) in combination with ejector

25 diluter (ED). Figure based on Jokiniemi *et al.* (2008).

26



27

28 **Fig. S3.** One stage dilution system: Dekati axial diluter (DAD 100). Figure based
29 on Dekati (2010).

30

31 ***Particle mass size distributions***

32 Analogous to the number distribution, the particle mass size distribution expresses the mass of
33 the particles within a size interval divided by the logarithmic range of the size interval
34 ($dm / d \log D_p$ on vertical axis) at the geometric mean of each size interval (D_p on horizontal axis).
35 This distribution is not measured directly but rather calculated with the ELPI+ results using the
36 estimated particle density of $\rho = 2.0 \text{ g cm}^{-3}$ and assuming spherical particles. Although the
37 particle number size distribution is more appropriate to relate particulate emissions to its health
38 impact, the particle mass size distribution can also be useful to compare both dilution systems,
39 especially for the particle fractions with the largest particles.

40 However, the sampling was not isokinetic since the flue gas velocity in the chimney is higher
41 than the sampling velocity so caution is necessary for drawing conclusions for coarse particles.
42 The maximum sampling error that occurs due to anisokinetic sampling is estimated to be lower
43 than 0.5% for $D_p < 0.1 \mu\text{m}$ when using the method described by Belyaev and Levin (1974). For
44 particles of $1 \mu\text{m}$ this error is estimated to be 2.2% at the lowest DR but reaches 22% at the
45 highest DR. For particles of $10 \mu\text{m}$ the error is estimated to be 95% at the lowest DR and almost a
46 tenfold of this for the highest DR. Furthermore, Pagels *et al.*, (2005) found that the original ELPI
47 overestimates the coarse mode which is likely due to fine particle losses (i.e. secondary particle
48 collection) which can result in non-negligible mass in the upper stages. They concluded that the
49 ELPI can give reliable high time- and size-resolved mass size distributions up to $3 \mu\text{m}$. Järvinen

50 *et al.* (2014) found that the new ELPI+ had a similar secondary collection of nanoparticles than
51 the ELPI for stages with the largest cut-off diameters. In addition, almost all coarse particles are
52 trapped by the multi-cyclone as the particles with $D_p > 2.5 \mu\text{m}$ only represent less than 0.04% of
53 the total number of particles in this study. For these reasons, only particles with $D_p < 3 \mu\text{m}$ are
54 considered here in the particle mass size distribution, namely stages 1 to 11.

55 In Fig. S4 and S5 the particle mass size distributions with the two dilution systems at various
56 tests are presented. With both dilution systems and during all operation modes, an accumulation
57 mode can be distinguished between 0.1 and 1 μm , which is in line with previous studies
58 regarding the particle mass size distribution of wood combustion (Lamberg *et al.*, 2011; Tissari *et al.*
59 *al.*, 2008b; Krugly *et al.*, 2014; Hays *et al.*, 2003; Wierzbicka *et al.*, 2005; Lillieblad *et al.*, 2004).
60 During some tests a second mode can be distinguished in the coarse fraction of the particle mass
61 size distributions which was also observed in previous studies (Lamberg *et al.*, 2011; Tissari *et al.*,
62 2008a,b). However, by only considering particles with $D_p < 3 \mu\text{m}$ this mode is not fully covered.
63 Note that the mass of particles in the size fractions with the smallest particles is negligibly small
64 since the mass varies with the diameter of the particles cubed. In addition, due to the same reason,
65 a small number of particles in the largest size fractions result in a high particle mass
66 concentration.

67 In Fig. S4a the average of the particle mass size distributions for the two dilution systems
68 during high load and low load are presented. The high load distributions are the averages of tests
69 S1.1 to S1.5 for both dilution systems. The low load distribution with the PTD + ED is the
70 average of tests S2.6 to S2.9 that were carried out with the overloaded ELPI+ impactor. The low
71 load distribution with the DAD 100 is the average of tests S2.8 and S2.9. With the DAD 100 both
72 distributions are quite similar although the low load distribution appears to be slightly lower.
73 With the PTD + ED high load distribution, the accumulation peak appears to be higher compared
74 to the DAD 100. Also, stage 9 is higher and stage 8 is lower than expected. By studying the
75 particle mass size distributions of the individual tests, it was observed that as time goes on, the
76 particle concentration in stage 9 increases and the concentration in stage 8 decreases. This is
77 probably due to a change in cut-off diameter of stage 9 resulting in the particles of stage 8 being
78 prematurely measured in stage 9. With the PTD + ED low load distribution, the accumulation
79 mode is higher and appears to be slightly shifted towards larger particles.

80 In Fig. S4b the particle mass size distribution of test S2.1 with both dilution systems is drawn.
81 Although this is the same operation mode as the high load in Fig. S4a, there are differences.
82 During test S2.1 with the DAD 100, the peak of the accumulation mode is less pronounced and a
83 small increase in the coarse fraction can be observed. With the PTD + ED no grease was used

84 during this test. The accumulation mode appears to be higher and an increase in the coarse
85 fraction can be observed.

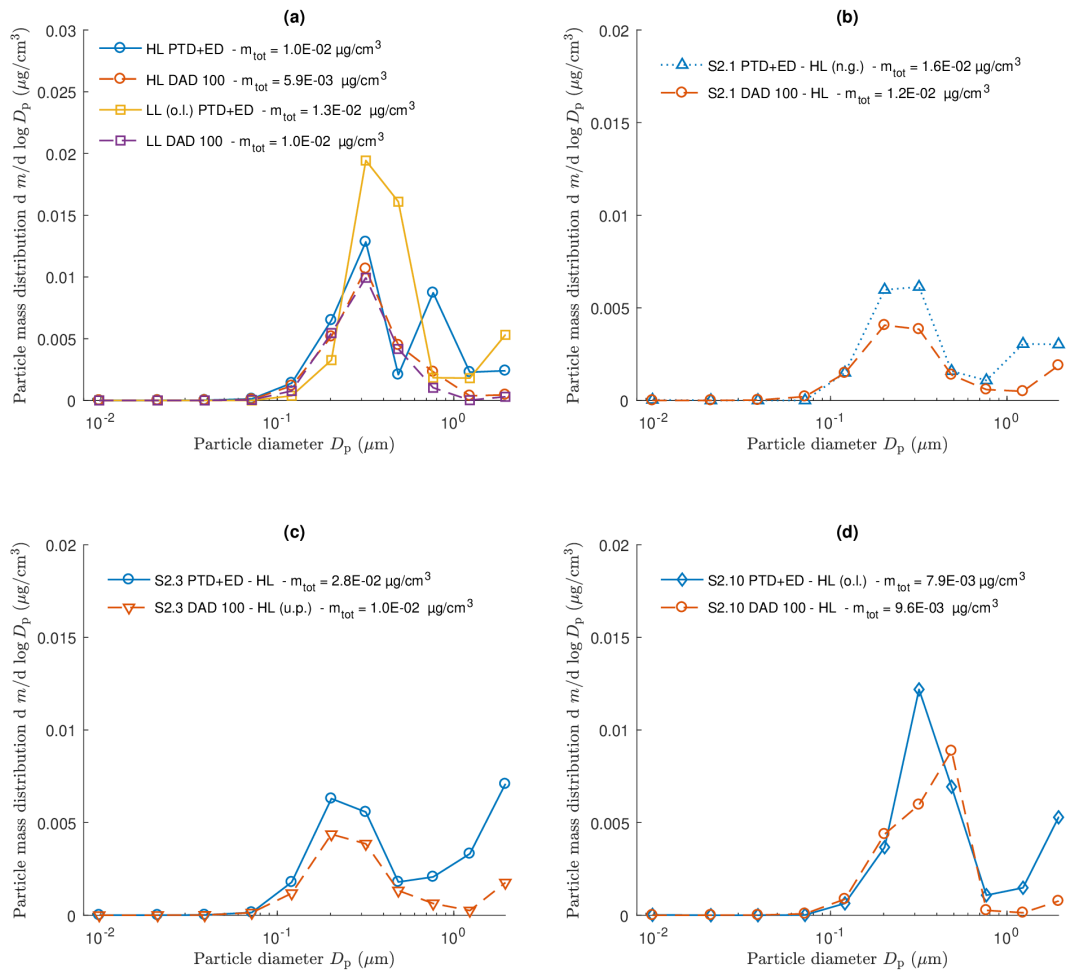
86 In Fig. S4c the particle mass size distribution of test S2.3 with both dilution systems is
87 presented. With the DAD 100 there was an unstable pressure in the ELPI+, but the distribution
88 appears to be similar to the distribution of tests S2.1. With the PTD + ED grease was used during
89 this tests but the distribution is similar to the distribution of tests S2.1 without grease. Only
90 stage 11 during S2.3 appears to be higher.

91 In Fig. S4d the particles mass size distribution of test S2.10 is shown for both dilution systems.
92 The test with the PTD + ED was measured with an overloaded ELPI+ impactor. The height of the
93 accumulation mode is similar as the one of the average high load tests in Fig. S4a. With the
94 DAD 100, the peak is more toward larger particles.

95 In Fig. S5 the particle mass size distributions are shown of the tests during high load with the
96 baghouse bypassed. During these tests, both ELPI+ impactors were overloaded with particles.
97 The peak of the accumulation mode appears to be lower for the DAD 100 compared with the
98 PTD + ED. With the PTD + ED, all tests show a shoulder in the coarse fraction while this is not
99 the case with the DAD 100.

100

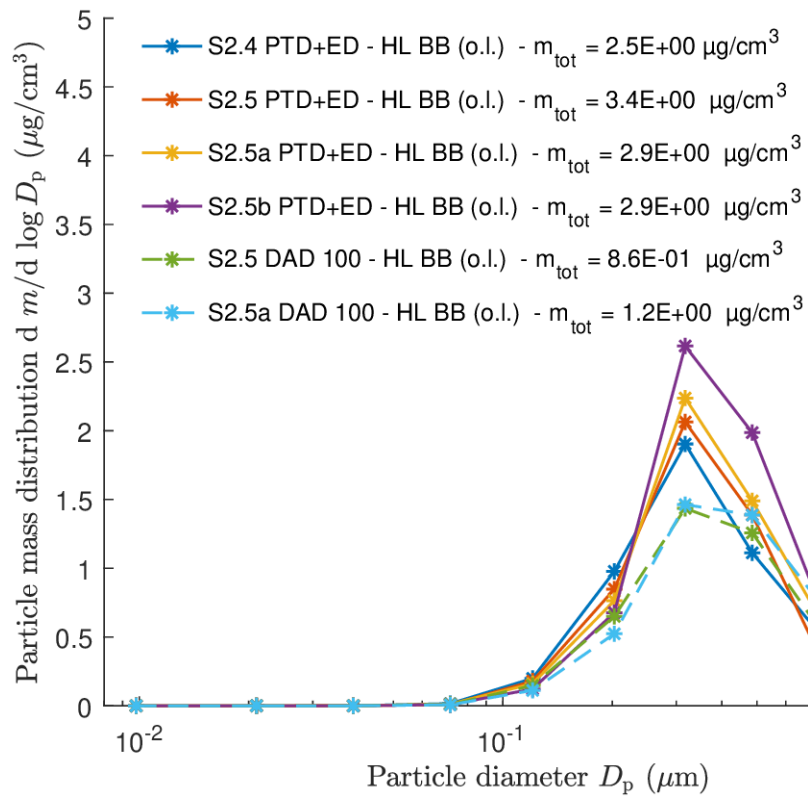
101



102

103 **Fig. S4.** Particle mass size distributions during high load (HL) and low load (LL) with both
 104 dilution systems. (a) HL are the average of tests S1.1 to S1.5. LL with PTD + ED is the average
 105 of tests S2.6 to S2.9 and measured with the ELPI+ impactor overloaded (o.l.). LL with DAD 100
 106 is the average of tests S2.8 and S2.9. (b) Simultaneous tests with no grease (n.g.) applied with
 107 ELPI+ A. (c) Simultaneous tests with unstable pressure (u.p.) is ELPI+ B. (d) Simultaneous tests
 108 with impactor of ELPI+ A overloaded (o.l.).

109



110

111 **Fig. S5.** Particle mass size distributions during high load with bypass of the baghouse with both

112 dilution systems.

113

114 *Alternative reasons for correlation between DR and particle concentration in stage 1*

115 The correlation could also be explained by various other processes, both measurement artefact
116 and aerosol dynamic related, of which some will be discussed here but these are believed to be
117 less likely or unlikely.

118 (i) A possible explanation is that DR was incorrectly estimated. This is however unlikely since
119 an incorrect DR would also cause a correlation with N_{tot} . Moreover, the good agreement of $N_{0.1-1}$
120 between different tests and the different dilution systems (e.g. see Fig. 2) indicates that DR is
121 indeed estimated correctly.

122 (ii) Another explanation is that the estimated particle density of 2.0 g cm^{-3} would induce such a
123 change in the size distribution causing stage 1 to correlate with DR. However, the same
124 correlation can be found when using a density of 1.0 g cm^{-3} since a change in density causes a
125 rescaling of the distribution rather than a distortion.

126 (iii) Another possibility is the correction algorithm of the ELPI+ that corrects the lower stages
127 for particle loss in the higher stages. However, investigation of the uncorrected data showed that
128 the correlation is present even without the correction. The corrected number concentration in
129 stage 1 is about 2.7 times the uncorrected concentration for all high load tests. This correction
130 factor depends on the currents measured in the higher stages and is almost constant during the
131 same operation mode. This correction factor is around 3.1 during the baghouse bypass and 2.7
132 during low load and changes little with the chosen particle density.

133 (iv) The correlation could be the result of increasing particle diffusional losses in the sampling
134 system with decreasing DR. Diffusion losses increase with increasing tube length, decreasing
135 particle size and decreasing flow rate (Brockmann, 2011). The tubes from the dilution systems to
136 the ELPI+'s were approximate 1 m and did not change with DR. Smaller particles will deposit
137 easier due to diffusion but there is no indication that particles reduce in size with decreasing DR.
138 The total flow rate in the DAD 100 is constant and does not change with DR. The flow rate in the
139 PTD decreases with decreasing DR which would result in an increase in diffusion losses,
140 however, due to the construction of the PTD particle deposition is minimized. The dilution ratio
141 of the ED is about constant and independent of the flow rate in the ED. Thus, the flow rate in the
142 ED does not correlate with the total DR. Therefore, it is rather unlikely that the correlation
143 between DR and the particle concentration in stage 1 is the result of increased diffusion
144 deposition with decreasing DR.

145 (v) The significant correlation observed between DR and particles in stage 1, could be the
146 result of the formation of new particles by increased nucleation with increasing DR. The dynamic
147 behavior of the gas-particle system in the dilution process will determine the number size
148 distribution after dilution and cooling (Lyyräinen *et al.*, 2004). Research on diesel particle
149 emissions has shown that the nuclei mode is subjected to dilution conditions (Kittelson *et al.*,
150 2006). It has been observed with diesel emissions that increasing dilution favors the formation of

151 particles with $D_p < 0.05 \mu\text{m}$ (Shi and Harrison, 1999; Shi *et al.*, 2000) but also a decrease of
152 nanoparticles with increasing dilution has been reported in literature (Jaiprakash *et al.*, 2016;
153 Suresh and Johnson, 2001; Abdul-Khalek *et al.*, 1999; Lipsky and Robinson, 2006). With diesel
154 exhaust, nucleation is possible because the nucleating species (mainly sulfuric acid and
155 hydrocarbons) are generally in the vapour phase in the tailpipe, and undergo a gas-to-particle
156 conversion during dilution and cooling (Kittelson *et al.*, 2006). With biomass combustion, only a
157 limited amount of gaseous species relevant for gas-to-particle conversion are present in the flue
158 gas at 150°C. At these conditions, probably only Na_2SO_4 , HCl and ZnCl_2 and less likely PbCl_2
159 can be expected (Jöller *et al.*, 2005). Also organic vapours can be expected in the flue gas but
160 only in low concentrations due to the high combustion efficiency. Nucleation of new particles is a
161 competing process with adsorption and condensation on pre-existing particles (Lyyräinen *et al.*,
162 2004). Therefore, besides nucleation, also condensation should occur since the particles in the
163 accumulation mode provide surface to condense on. There is however no positive significant
164 correlation with DR and particle concentration in the accumulation mode (see Table 3). Moreover,
165 the opposite was observed in Fig. 7, with decreasing DR the peak of the accumulation mode
166 shifted to larger particles sizes. In addition, nucleation of new particles requires a large saturation
167 ratio (Hinds, 2011). Since with the PTD + ED the dilution occurs in two stages (i.e. first
168 decreasing the vapour pressure and then decreasing the temperature), the flue gas is not expected

169 to become supersaturated during dilution and thus nucleation of new particles in the dilution

170 system is not likely.

171

172 ***Sampling time until impactor overload***

173 The sampling time until particle overload in the impactors can be estimated based on the
174 dilution ratio and the actual measured distributions. The maximum particle load given by the
175 ELPI+ user manual is 1 mg (Dekati, 2016). However, van Gulijk *et al.* (2001) showed that after
176 collecting only 15 µg of particles, the relative error on the measured particle number size
177 distribution is already 10% due to the prematurely measuring of small particles. In Table S1, the
178 sampling time until overload is given for both maximum particle loads (i.e. $m_{\max} = 1$ mg and
179 15 µg). The column *accum. mode* indicates the time until at least one impactor stage of the
180 accumulation mode reaches the maximum particle load. Analogue, the column *coarse mode*
181 indicates the time until at least one impactor stage of the coarse mode reaches the maximum
182 particle load. The sampling times are estimated for high boiler load without baghouse bypass (HL)
183 and for high boiler load with baghouse bypass (HL BB) and for three different dilution ratios.
184 The dilution ratios are the typical DR of the DAD 100 dilution system (DR = 10), the
185 recommended DR for the PTD + ED dilution system (DR = 20) and a high DR of 1000 (by
186 extrapolating the estimations of DR = 20).

187 Both dilution systems can be used at least 13 h to sample emissions during HL before one
188 of the impactor stages reaches 1 mg and needs cleaning. However, after only about 12 minutes of
189 sampling the relative errors become larger than 10% due to the prematurely measuring of the
190 smallest particles.

191 Both dilution systems can be used less than 4 minutes to sample emissions during HL BB
 192 before one of the impactor stages reaches 1 mg and needs cleaning. After less than 4 s the relative
 193 errors become larger than 10%. Using a dilution system with DR = 1000 would extend the
 194 sampling time before overload to over 2 h but after less than 2 minutes the relative error would
 195 exceed 10%. In any case, keeping the relative error below 10% by limiting the sampling time is a
 196 rather inconvenient method for carrying out measurements.

197 It is recommend to take this dynamic behavior of impactors into account when designing
 198 an experiment and to relate the particle load on the impactors with the obtained concentrations
 199 when interpreting the results.

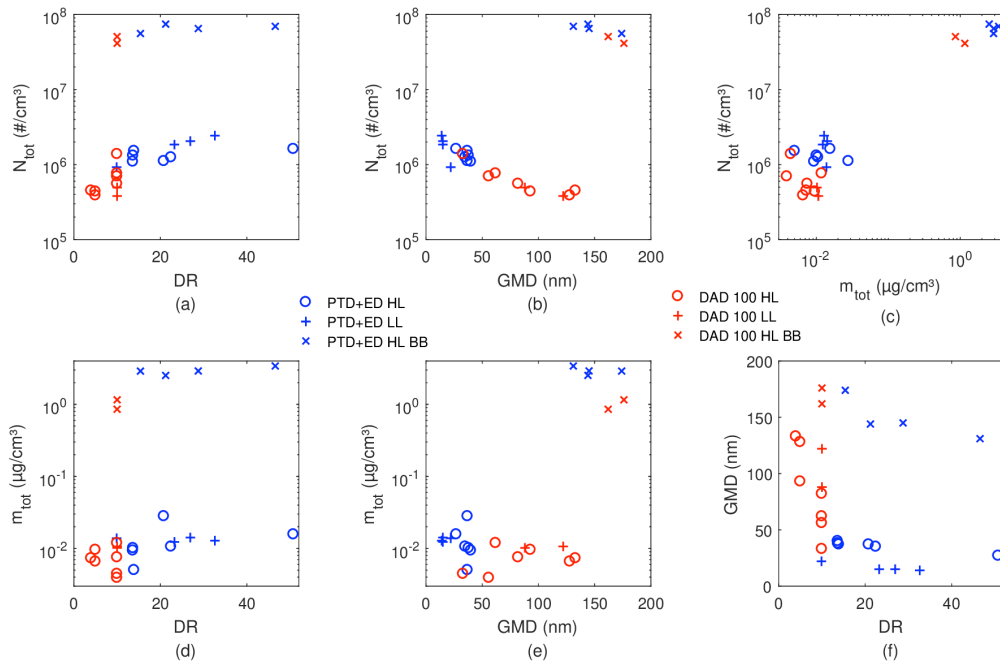
200

201 **Table S1.** Sampling time until at least one impact stage is overloaded.

Load	Dilution system	DR	$m_{\max} = 1 \text{ mg}$		$m_{\max} = 15 \text{ }\mu\text{g}$	
			accum. mode	coarse mode	accum. mode	coarse mode
HL	DAD 100	10	13.9 h	75.3 h	12.5 min	67.8 min
	PTD + ED	20	20.8 h	13.3 h	18.8 min	12.0 min
		1000	1040 h	667 h	938 min	600 min
HL BB	DAD 100	10	3.7 min	20.0 min	3.3 s	18.0 s
	PTD + ED	20	6.8 min	2.5 min	6.1 s	2.3 s
		1000	341 min	126 min	307 s	113 s

202

203



204

205 **Fig. S6.** The mutual relations between total particle number N_{tot} , total particle mass m_{tot} ,

206 geometric mean particle diameter GMD and dilution ratio DR. HL: high load, LL: low load, HL

207 BB: high load with baghouse bypassed.

208

209 **REFERENCES**

210

211 Abdul-Khalek, I., Kittelson, D. and Brear, F. (1999). The influence of dilution conditions on
212 diesel exhaust particle size distribution measurements. *SAE Transactions* 108: 563-571.

213 Belyaev, S.P. and Levin, L.M. (1974). Techniques for collection of representative aerosol
214 samples. *J. Aerosol Sci.* 5: 325-338.

215 Brockmann, J.E. (2011). In *Aerosol measurement: Principles, techniques, and applications*,
216 Kulkarni, P., Baron, P.A. and Willeke, K. (Eds.), Wiley, Hoboken, New Jersey, Chapter 6, p.
217 69-105.

218 Dekati (2010). Dekati axial diluter DAD-100. User Manual ver. 2.0. Dekati Ltd., Tampere,
219 Finland.

220 [Dekati \(2016\). Dekati ELPI+. User Manual ver. 1.54. Dekati Ltd., Tampere, Finland.](#)

221 Hays, M.D., Smith, N.D., Kinsey, J., Dong, Y. and Kariher, P. (2003). Polycyclic aromatic
222 hydrocarbon size distributions in aerosols from appliances of residential wood combustion as
223 determined by direct thermal desorption - GC/MS. *J. Aerosol Sci.* 34: 1061-1084.

224 Hinds, W.C. (2011). In *Aerosol measurement: Principles, techniques, and applications*, Kulkarni,
225 P., Baron, P.A. and Willeke, K. (Eds.), Wiley, Hoboken, New Jersey, Chapter 3, p. 31-40.

226 Jaiprakash, Habib, G. and Kumar, S. (2016). Evaluation of portable dilution system for aerosol

227 measurement from stationary and mobile combustion sources. *Aerosol Sci. Tech.*50: 717-731.

228 Järvinen, A., Aitomaa, M., Rostedt, A., Keskinen, J. and Yli-Ojanperä, J. (2014). Calibration of
229 the new electrical low pressure impactor (ELPI+). *J. Aerosol Sci.* 69: 150-159.

230 Jokiniemi, J., Hytönen, K., Tissari, J., Obernberger, I., Brunner, T., Bärnthaler, G., Friesenbichler,
231 J., Salonen, R.O., Hirvonen, M.R., Jalava, P., Pennanen, A., Happonen, M., Vallius, M.,
232 Markkanen, P., Hartmann, H., Turowski, P., Roßmann, P., Ellner-Schubert, F., Boman, C.,
233 Pettersson, E., Wiinikka, H., Hillamo, R., Saarnio, K., Frey, A., Saarikoski, S., Timonen, H.,
234 Teinilä, K., Aurela, M., Sillanpää, M., Bellmann, B., Sandström, T., Sehlstedt and M.,
235 Forsberg, B. (2008). Biomass combustion in residential heating: Particulate measurements,
236 sampling, and physicochemical and toxicological characterisation. Technical Report.
237 University of Kuopio, ERA-NET Bioenergy Program.

238 Jöller, M., Brunner, T. and Obernberger, I. (2005). Modeling of aerosol formation during biomass
239 combustion in grate furnaces and comparison with measurements. *Energ. Fuel.* 19: 311-323.

240 Kittelson, D.B., Watts, W.F. and Johnson, J.P. (2006). On-road and laboratory evaluation of
241 combustion aerosols - Part 1: Summary of diesel engine results. *J. Aerosol Sci.* 37: 913-930.

242 Krugly, E., Martuzevicius, D., Puida, E., Buinevicius, K., Stasiulaitiene, I., Radziuniene, I.,
243 Minikauskas, A. and Kliucininkas, L. (2014). Characterization of gaseous- and particle-phase
244 emissions from the combustion of biomass-residue-derived fuels in a small residential boiler.

245 *Energ. Fuel.* 28: 5057-5066.

246 Lamberg, H., Nuutinen, K., Tissari, J., Ruusunen, J., Yli-Pirilä, P., Sippula, O., Tapanainen, M.,
247 Jalava, P., Makkonen, U., Teinilä, K., Saarnio, K., Hillamo, R., Hirvonen, M.R. and Jokiniemi,
248 J. (2011). Physicochemical characterization of fine particles from small-scale wood
249 combustion. *Atmos. Environ.* 45: 7635-7643.

250 Lillieblad, L., Szpila, A., Strand, M., Pagels, J., Rupar-Gadd, K., Gudmundsson, A., Swietlicki,
251 E., Bohgard, M. and Sanati, M. (2004). Boiler operation influence on the emissions of
252 submicrometer-sized particles and polycyclic aromatic hydrocarbons from biomass-fired grate
253 boilers. *Energ. Fuel.* 18: 410-417.

254 Lipsky, E.M. and Robinson, A.L. (2006). Effects of dilution on fine particle mass and
255 partitioning of semivolatile organics in diesel exhaust and wood smoke. *Environ. Sci. Technol.*
256 40: 155-162.

257 Lyyränen, J., Jokiniemi, J., Kauppinen, E.I., Backman, U. and Vesala, H. (2004). Comparison of
258 different dilution methods for measuring diesel particle emissions. *Aerosol Sci. Tech.* 38: 12-23.

259 Pagels, J., Gudmundsson, A., Gustavsson, E., Asking, L. and Bohgard, M. (2005). Evaluation of
260 aerodynamic particle sizer and electrical low-pressure impactor for unimodal and bimodal
261 mass-weighted size distributions. *Aerosol Sci. Tech.* 39: 871-887.

- 262 Shi, J.P. and Harrison, R.M. (1999). Investigation of ultra fine particle formation during diesel
263 exhaust dilution. *Environ. Sci. Technol.* 33: 3730-3736.
- 264 Shi, J.P., Mark, D. and Harrison, R.M. (2000). Characterization of particles from a current
265 technology heavy-duty diesel engine. *Environ. Sci. Technol.* 34: 748-755.
- 266 Suresh, A. and Johnson, J.H. (2001). A study of the dilution effects on particle size measurement
267 from a heavy-duty diesel engine with EGR. *SAE Transactions* 110: 337-346.
- 268 Tissari, J., Lyyräinen, J., Hytönen, K., Sippula, O., Tapper, U., Frey, A., Saarnio, K., Pennanen,
269 A., Hillamo, R., Salonen, R., Hirvonen, M.R. and Jokiniemi, J. (2008a). Fine particle and
270 gaseous emissions from normal and smouldering wood combustion in a conventional masonry
271 heater. *Atmos. Environ.* 42: 7862-7873.
- 272 Tissari, J., Sippula, O., Kouki, J., Vuorio, K. and Jokiniemi, J. (2008b). Fine particle and gas
273 emissions from the combustion of agricultural fuels fired in a 20 kW burner. *Energ. Fuel.* 22:
274 2033-2042.
- 275 van Gulijk, C., Schouten, J.M., Marijnissen, J.C.M., Makkee, M. and Moulijn, J.A. (2001).
276 Restriction for the ELPI in diesel particulate measurements. *J. Aerosol Sci.* 32: 1117-1130.
- 277 Wierzbicka, A., Lillieblad, L., Pagels, J., Strand, M., Gudmundsson, A., Gharibi, A., Swietlicki,
278 E., Sanati, M. and Bohgard, M. (2005). Particle emissions from district heating units operating

279 on three commonly used biofuels. *Atmos. Environ.* 39: 139-150.

280